BBA-Bioenergetics special issue on

"Vibrational Spectroscopies and Bioenergetic Systems"

Infrared spectroscopic studies on the V-ATPase

Hideki Kandori[a, b], Yuji Furutani[c, d] and Takeshi Murata[e, f]

[a]Department of Frontier Materials, Nagoya Institute of Technology, Showa-ku, Nagoya 466-8555, Japan, [b]OptoBioTechnology Research Center, Nagoya Institute of Technology, Showa-ku, Nagoya 466-8555, Japan, [c]Department of Life and Coordination-Complex Molecular Science, Institute for Molecular Science, 38 Nishigo-Naka, Myodaiji, Okazaki 444-8585, Japan, [d]Department of Structural Molecular Science, The Graduate University for Advanced Studies (SOKENDAI), 38 Nishigo-Naka, Myodaiji, Okazaki 444-8585, Japan, [e]PRESTO, Japan Science and Technology Agency (JST), 4-1-8 Honcho Kawaguchi, Saitama 332-0012, Japan, [f]Department of Chemistry, Graduate School of Science, Chiba University, 1-33 Yayoi-cho, Inage, Chiba 263-8522, Japan

*Address correspondence to: Hideki Kandori, kandori@nitech.ac.jp

Abstract

V-ATPase is an ATP-driven rotary motor that vectorially transports ions. Together with F-ATPase, a homologous protein, several models on the ion transport have been proposed, but their molecular mechanisms are yet unknown. V-ATPase from *Enterococcus hirae* forms a large supramolecular protein complex (total molecular weight: ~700,000) and physiologically transports Na^+ and Li^+ across a hydrophobic lipid bilayer. Stabilization of these cations in the binding site has been discussed on the basis of X-ray crystal structures of a membrane-embedded domain, the K-ring (Na^+ and Li^+ bound forms). Sodium or lithium ion binding-induced difference FTIR spectra of the intact *E. hirae* V-ATPase have been measured in aqueous solution at physiological temperature. The results suggest that sodium or lithium ion binding induces the deprotonation of Glu139, a hydrogen-bonding change in the tyrosine residue and rigid α-helical structures. Identical difference FTIR spectra between the entire V-ATPase complex and K-ring strongly suggest that protein interaction with the I subunit does not cause large structural changes in the K-ring. This result supports the previously proposed Na^+ transport mechanism by V-ATPase stating that a flip-flop movement of a carboxylate group of Glu139 without large conformational changes in the K-ring accelerates the replacement of a Na^+ ion in the binding site.

Keywords

V_1/V_o-ATPase, ATR-FTIR spectroscopy, X-ray crystallography, sodium binding, hydrogen bond, protonation, conformation change

Contents

1 Introduction

2 X-ray structure of V-ATPase from *Enterococcus hirae*

3 ATR FTIR spectroscopy of membrane proteins

4 ATR-FTIR study of V-ATPase

4-1. ATR-FTIR difference spectra of the entire V-ATPase complex

4-2. ATR-FTIR difference spectra of the K-ring

5 Mechanistic insights from X-ray structure and vibrational spectroscopy

6 Conclusion and perspective

7 Acknowledgements

1 Introduction

Biological systems contain various active transport machineries, where uni-directional transports of ions and substrates are achieved across the membrane [1-6]. Mechanism of such molecular machineries is one of the central questions in bioenergetics. Transporters and pumps are membrane proteins, which include specific pathway of ions and substrates. However, the pathways cannot be fully connected between the two sides of the membrane, because the gradient formed by active transport will be collapsed. This is an important aspect in distinguishing transporters and pumps from channels. The former needs energy input, which ensures the uni-directionality of transport across the membrane. Light and chemical energy by specific chemical reactions are used to drive these molecular machines. In particular, the energy gained by ATP hydrolysis is ubiquitously used in biological systems.

V-ATPases couple ion movement with ATP hydrolysis, whose structure and mechanism resemble those of F-ATPases [7]. V-ATPases have a globular catalytic domain, V_1 (equivalent to F_1), where ATP is hydrolyzed. This domain is attached by central and peripheral stalks to the intrinsic membrane domain, V_o (equivalent to F_o), which pumps ions across the membrane. It is generally accepted that electrostatic interaction at the glutamate (asparatate) residues within the H^+ (or Na^+)-binding sites of the c-ring and the conserved arginine residue of the a-subunit of V_o (or F_o) is crucial for ion-transport mechanism. Several ion transporting mechanism models of F-ATPases have been reported before

obtaining the precise structure of the F_o part. First, Junge *et al.* have proposed 'two-half-channel' model [8]. In the ion pumping mode, rotation of the c-ring by ATP hydrolysis energy via F_1-ATPase brings an occupied ion-binding site into the interface between c-ring and a-subunit. The a-subunit provides for 'exit' and 'entry' of the ions via aqueous half-channels to periplasm and from cytoplasm, respectively (Fig. 1a). Second, NMR studies of the monomeric c-subunit in organic solvent mixtures at various pH values have suggested that the process of pumping ions involves large conformational changes which involve swiveling of the outer helix of subunit c of *E. coli* F-ATPase (Fig. 1b) [9]. Third, 'single channel' model has also been proposed for the F-ATPase from *Propioniogenium modestum*, where the Na^+-binding site is placed close to the membrane center, but Na^+ can exchange through an intrinsic c-ring channel connecting the ion-binding sites to the cytoplasm (Fig. 1c) [10]. In the pumping mode, the bound ion of the c-ring release at a half-channel to periplasm of a-subunit between the interfaces. Recent progresses suggest that the 'two-half-channel' model without swiveling of the helix of c-ring is most favorable [11, 12], but the precise mechanism of ion translocation by F (or V)-ATPase remains unclear because of the lack of the atomic structure of the membrane protein complex.

V-ATPase from *Enterococcus hirae* physiologically transports Na^+ and Li^+ [13]. This enzyme is encoded by nine *ntp* genes (*ntp*FIKECGABD) organized in the *ntp* operon [14]. Amino acid sequences of NtpF, -I, -K, -E, -C, -G, -A, -B, and -D were homologous with those

of the subunits G, a, c, E, d, F, A, B, and D of eukaryotic V-ATPases, respectively [15]. The V_1 domain responsible for ATP-driven rotation consists of the Ntp-A, -B, -C, -D, -E, and -G subunits (Fig. 2). In V_1, the three A subunits and the three B subunits are arranged alternately around a central D subunit. V_o domain, which utilizes the rotation of V_1 for the transport of Na^+ (or Li^+), is composed of oligomers of 16-kDa NtpK, which form a membrane rotor ring (K-ring), and a single copy of the NtpI subunit. The V_1 and V_o domains are connected by a central stalk, which is composed of NtpD, NtpG, and NtpC subunits, and two peripheral stalks, which are composed of NtpE and NtpF subunits of V_1. ATP hydrolysis induces the rotation of the central stalk and the attached K-ring, which causes Na^+ (or Li^+) pumping at the interface between the K-ring and NtpI subunit.

2 X-ray crystal structures of membrane rotor K-ring of *Enterococcus hirae* V-ATPase

In 2005, the crystal structure of the Na^+-bound K-ring was reported as the first high-resolution ring structure (Fig. 3a and b) [16]. Ten sodium ions are bound to the specific binding pockets each of which is composed of five oxygen atoms 2.2-2.3 Å distant, four of them in the side chains of T^{64}, Q^{65}, Q^{110} and E^{139}, and the fifth in the main chain carbonyl of L^{61}. They are located on the external surface of the ring, and the hydrophobic surface arrangement places the Na^+-binding site close to the center of the bilayer. Recently, the

crystal structure of the Li^+-bound K-ring was also reported (Fig. 3c) [17]. The overall structure of the Li^+-bound K-ring is almost identical (RMSD for all atoms; 0.09 Å) to that of Na^+ bound K-ring except for the ion binding pocket of each K-subunit (Fig. 3b and c). Each Li^+ is surrounded by five oxygen atoms in Helix 2, 3 and 4 all contribute to the Li^+-binding pocket as seen in the Na^+ bound K-ring structure. The distances between Li^+ and the oxygen atoms are slightly shorter than those between Na^+ and the oxygen atoms. Thus, the ion binding pocket of the K-ring specifically binds Na^+ or Li^+ using identical binding pocket with slightly different metal – oxygen distances.

The ion transport mechanism has been discussed on the basis of these structures; however, X-ray crystal structures lack information on hydrogen atoms. Of the five residues involved in Na^+ binding to the K-ring only one, an essential glutamate (E^{139}) is conserved in all H^+-transporting V-ATPases. The other four residues (L^{61}, T^{64}, Q^{65} and Q^{110}) are not conserved. It is widely accepted that the H^+ binding/release in H^+ transport of V-ATPase occurs via protonation/deprotonation of the carboxyl group of the glutamate residue. The K-ring whose carboxyl group should be protonated at acidic pH does not bind $^{22}Na^+$ with the same high affinity at alkali pH. Analysis of inhibition by H^+ ions suggested that the K-ring binds Na^+ and H^+ competitively [17]. The K_i value of H^+ corresponds to the acid dissociation constant (K_a) of the E^{139}, the pK_a of which is 5.5. However, we have not observed ATP-driven H^+ uptake activity into proteoliposomes reconstituted with the whole

V-ATPase complex at pH 5.5 in the effective absence of Na^+. It proved impossible to obtain crystals of H^+ bound K-ring under acidic conditions, as the K-ring was unstable at less than pH 4.5. Therefore, precise structural differences such as protonation states of carboxylate residues and hydrogen-bonding structures of amino-acid side chains remained unclear.

3 ATR FTIR spectroscopy of membrane proteins

Stimulus-induced difference Fourier-transform infrared (FTIR) spectroscopy is a powerful tool to investigate protein structural changes accompanying biologically important functional processes. This method has been extensively applied to photo-active proteins [18-21], and has been shown to allow detailed structural analysis including changes in hydrogen-bonding of even a single water molecule [22-24]. However, this technique has not been easily applied for other stimuli such as ion- and ligand-binding. Attenuated Total Reflection (ATR)-FTIR spectroscopy uses samples that are filled in aqueous solution, so that solution pH, ionic and molecular composition can be preserved and accurately controlled [25-27]. Consequently, ion- and ligand-binding induced difference ATR-FTIR spectra provided the atomic-detailed mechanisms of membrane proteins to stimuli, as for respiratory cytochrome bc_1 complex [28], cytochrome *c* oxidase [29-31], gastric ATPase [32], nicotinic acetylcholine receptor [33-35], Na^+/galactose transporter [36], oligopeptide transporter [37], transhydrogenase [38, 39], melibiose permease [40-42], microbial rhodopsins (they are

photoreceptive proteins, but ion-binding was measured by ATR-FTIR spectroscopy in these papers) [43-45], flagellar motor PomA-PomB complex [46], and potassium channel KcsA [47].

In ion- and ligand-binding induced difference FTIR spectroscopy, the samples were physically adsorbed on an attenuated total reflection (ATR) crystal and soaked in a buffer solution containing ions at a concentration suitable for the investigation of the ion binding site (depending on the K_D values). It should be noted that "physical adsorption" does not require any special treatment for samples in case of membrane proteins. In case of soluble proteins and membrane proteins solubilized by detergents, samples are easily detached from the ATR cells upon buffer exchange. In contrast, weak interaction between membrane proteins in lipids and ATR cell surface is sufficient for adsorption during measurements.

We thus applied ion-binding induced difference ATR-FTIR spectroscopy to V-ATPase (total molecular weight: ~700,000) [48], which was the largest protein complex by ATR-FTIR spectroscopy. Experimental setup is shown in Fig. 4. The V-ATPase sample of the entire complex or the purified K-ring was placed on the surface of a diamond ATR crystal with nine effective internal reflections (DurasamplIR II, Smiths Detection, UK). After drying in a gentle stream of N_2, the sample was rehydrated with perfusion buffer (20 mM Bis-Tris at pH 6, 2.5 mM $MgSO_4$, 8% Glycerol). The sample was covered by a glass jacket for maintaining the temperature and introducing buffer solutions to the sample (Fig. 4b). Before

measuring the Na^+-induced difference spectra, the film was perfused with the same buffer at a flow rate of 0.5 mL/min for 100 min. ATR-FTIR spectra of the V-ATPase sample were recorded at 293 K and 2 cm^{-1} resolution using a Bio-Rad FTS-6000 spectrometer, equipped with a liquid nitrogen-cooled MCT detector (Fig. 4a). Exchanging buffer solutions was regulated by a chromatography system with a computer-controlled solenoid valve (Gradicon III with one peristaltic pump, ATTO, Japan) (Fig. 4a and c). A background spectrum of the film (an average of 4560 interferograms) was first recorded during perfusion with buffer in the absence of NaCl for 40 min. The buffer was then switched to that containing 1 mM NaCl, and after a 5 min delay for equilibration, a Na^+-binding *minus* Na^+-free difference spectrum was recorded for 40 min (an average of 4560 interferograms). Then, the buffer was switched back to that without NaCl, and after a 5 min delay, an equivalent Na^+-free *minus* Na^+-binding difference spectrum was recorded with the spectrum collected just before as a new background. The cycling procedure was repeated six times, and the difference spectra were calculated as averages of [V-ATPase(Na^+) *minus* V-ATPase(free)] and [V-ATPase(free) *minus* V-ATPase(Na^+)] spectra. The flow rate was maintained at 0.5 mL/min. V-ATPase(Li^+) *minus* V-ATPase(free) spectra and V-ATPase(Na^+) *minus* V-ATPase(Li^+) were measured by the same method.

4 ATR-FTIR study of V-ATPase

4-1. ATR-FTIR difference spectra of the entire V-ATPase complex

Fig. 5 shows sodium- (a) and lithium ion (b) binding-induced difference infrared spectra measured in the buffer (20 mM Bis-Tris (pH 6), 2.5 mM $MgSO_4$, 8% glycerol) containing 1 mM NaCl or LiCl against the buffer without these salts as reference [48]. K_D values reported for Na^+ ($K_{D(Na+)}$) were 15 μM for the entire complex [49] and 12 μM for the K-ring [17]. Therefore, the spectral changes are considered to be caused by the binding of ions to the binding site. In fact, a similar Na^+ binding spectrum was obtained at 100 μM NaCl [48]. Li^+ affinity for the K-ring was examined by the inhibition assay and its K_i value was estimated to be 48 μM [17]. The concentration of LiCl (1 mM) was also sufficiently high. The difference spectra between sodium and lithium ion binding forms were also measured and compared with the spectrum calculated by subtracting the lithium-ion spectrum (Fig. 5b) from the sodium-ion spectrum (Fig. 5a). The spectra were very similar to each other (Fig. 5c), which indicates that the negative sides in (Fig. 5a) and (Fig. 5b) were completely canceled out by the subtraction.

After the ion-binding induced difference ATR-FTIR experiment, the stability of the entire V-ATPase complex was examined by SDS-PAGE (Fig. 6a) and Na^+-dependent ATPase activity (Fig. 6b). The band patterns obtained by SDS-PAGE were almost identical between before (lane 1) and after the experiment (lane 2) (Fig. 6a). A and B subunits are the main components of the V_1 domain and are relatively easily detachable from the complex; however,

they survived during the measurement. Not only the structure but also the function of V-ATPase was found to be retained as indicated by the result that at least 70% of the Na^+-dependent ATPase activity remained (Fig. 6b). Desorption of the sample from the ATR cell surface was estimated to be ~17% from the amide I intensity. Therefore, the substantial degeneration was limited to ~13% after the experiment, which insures that our ion binding-induced difference spectrum is obtained from the intact V-ATPase sample.

The negative bands at 1737 cm^{-1} in Fig. 5a and b correspond to the characteristic frequency of the C=O stretching vibration of a protonated carboxyl group of Asp or Glu. On the other hand, the positive bands at 1561 and 1422 cm^{-1} (Fig. 5a) and at 1563 and 1426 cm^{-1} (Fig. 5b) correspond to the characteristic frequency of antisymmetric and symmetric COO^- stretching vibrations of carboxylate groups. Therefore, these vibrational signals are likely to originate from carboxylate responsible for binding of sodium- and lithium-ions, where negative signals indicate proton binding. This is supported by the difference spectrum after the reaction with *N, N'*-dicyclohexylcarbodiimide (DCCD) (Fig. 5d, red), which binds to E^{139} in the K-ring and decreases the $K_{D(Na+)}$ value significantly [15].

The frequency difference between the antisymmetric and symmetric stretches of carboxylate depends on the interaction with the cation [50, 51]. A difference larger than 200 cm^{-1} indicates a monodentate structure, where only one C=O group interacts with the cation and the other is free. The differences in the Na^+- and Li^+-bound forms are 139 and 137 cm^{-1},

respectively (Fig. 5), and less than the criterion. According to the literature [50], the carboxylate group interacts with cations in the pseudo-bridging structure, where one C=O group interacts with a cation and the other interacts with water or another OH group. This is consistent with X-ray crystal structures (Fig. 3b and c), though the possibility of bidentate binding mode cannot be excluded from the frequencies.

The bands at 1512 and 1314 cm^{-1} (Fig. 5a) and at 1533 and 1330 cm^{-1} (Fig. 5b) exhibit frequency changes that depend upon the binding of sodium and lithium ions. These modes are characteristic to phenol ring stretching and phenol C-O stretching modes of tyrosine residues [52], though they were not assigned by isotope labeling. The frequency shift is more pronounced in the difference spectrum shown in Fig. 5c (1510/1532 and 1313/1330 cm^{-1}). The most probable candidate is Y^{68} in the K-ring. From X-ray crystal structures, the structural difference attributed to Y^{68} between the Na^{+}- and Li^{+}-bound forms is not clear, but the infrared spectra showed a significant effect due this residue. The cations do not directly interact with Y^{68}, but it may be important for the regulation of the electronic structure of E^{139} thorough the hydrogen bond. When the cations are removed from the binding site, E^{139} is protonated and the C=O stretching mode of carboxylic acid appears at 1737 cm^{-1}. The frequency suggests that E^{139} forms one moderate hydrogen bond with a polar side chain group [53], which implies that E^{139} keeps a hydrogen-bond with Y^{68} regardless of its protonation state.

The results in Fig. 5 clearly demonstrate that ion-binding induced difference ATR-FTIR spectroscopy successfully obtain structural changes upon binding of sodium-ions to V-ATPase, though V-ATPase is a large protein complex (total molecular weight: ~700,000). The most intense peaks in Fig. 5a were observed at 1666 (-)/1656 (+)/1641 (-) cm^{-1}, which are located in the amide I region consisting of a main chain carbonyl C=O stretches. Amide-I frequency depends on the secondary structure, and a positive peak at 1656 cm^{-1} is characteristic of α-helix. This indicates more α-helical content in the sodium-ion binding form than in the sodium-ion free (proton binding) form. It is likely that release of sodium ion loosens the structures of transmembrane α-helices.

4-2. ATR-FTIR difference spectra of the K-ring

To further gain structural information, we prepared K-ring alone, and applied ATR-FTIR spectroscopy to K-ring. Fig. 7 compares the difference spectra upon binding of sodium ions between native V-ATPase (red) and K-ring (blue). As is clearly seen, the two spectra are almost identical, being consistent with the above interpretation, because K-ring has the binding site of sodium ion. In the K-ring, there are two aspartate and four glutamate residues (D^{3}, E^{39}, E^{50}, D^{83}, E^{126}, and E^{139}). Among them, only E^{139} constitutes the sodium ion binding site. The other binding sites in the aqueous phase are on the cytoplasmic surface (E^{50} and E^{126}), on the extracellular surface (D^{3} and D^{83}), and in the inner ring (E^{39}). These

residues are easily accessible to bulk water at pH 6 and are always deprotonated independently of the presence of sodium or lithium ions. Therefore, these bands could reasonably be considered to originate from E^{139} residues in the K-ring.

ATP hydrolysis in the A_3B_3 domain drives the rotation of the central stalk (D, G, and C subunits) and the connected K-ring, which drives the pumping of Na^+ ions through the interface between the K-ring and the I subunit. In the presence of a Na^+ ion, E^{139} is deprotonated, which generates an ion pair in the binding site. It would be interesting to know whether such a drastic change in the electrostatic field of the binding site could induce some conformational changes in a K-ring unit. The amplitude of the positive peak of amide-I mode was 0.00046 at 1656 cm^{-1}, which corresponds to about 0.4% and 1.7% of the entire amide I band of the entire complex (0.11 a.u.) (Fig. 5a), and the K-ring (0.026 a.u. estimated from the ratio of the molecular weight between the entire complex, 698 kDa, and the K-ring, 160 kDa) (Fig. 7), respectively. One subunit of the K-ring consists of 156 amino acid residues and 1.7 % apparently corresponds to 2.7 residues. It should be noted that these values are obtained from difference spectra, in which positive and negative contributions are possibly canceled. This indicates the value (2.7 residues) is minimal and more amino acids should be involved in conformational changes.

From the spectral decomposition analysis in Fig. 8, we estimated the real number of amino acid residues participating in conformational changes upon ion binding as follows.

By subtracting water and buffer absorption, the absolute absorption spectrum of the entire V-ATPase complex was obtained and its amide-I band intensity was 0.11 (Fig. 8a). The contribution of the K-ring is estimated to be 0.026 from the molecular weight (0.11 × 160 kDa/698 kDa). The number of amino acids in one subunit of the K-ring is 156, which means that one amide group has 0.000017 and 10 homologous amide groups in 10 NtpK monomers in total have 0.00017. Estimation of the number of the amide groups that contribute to the Na^+ binding-induced difference spectrum was carried out by spectral decomposition of the Na^+ binding spectrum in the amide I region using two methods; the band narrowing of one component (Fig. 8b) and the frequency shifts of two components (Fig. 8c). In the former case, the amplitude of the negative band is 0.001; therefore, the number of amide groups is 5.9 (0.001/0.00017). In the latter case, the amplitude of the negative bands is 0.00083 in total; therefore, the number of amide groups is 4.9 (0.00083/0.00017). Therefore, upon binding of Na^+ or Li^+ ions, 5–6 amide groups form a rigid α-helix conformation.

We expected similar difference spectra upon binding of sodium ions between the entire V-ATPase complex (red spectrum in Fig. 7) and K-ring (blue spectrum in Fig. 7), and the results support the idea that the observed spectral changes monitor local conformational alteration in K-ring. Band assignments of 1737 (-), 1561 (+), 1422 (+) cm^{-1} (E^{139}) and 1512 (+), 1314 (+) cm^{-1} (Y^{68}) are also supported by the reproduced observation for K-ring. In addition, identical spectral features in amide-I bands provide important structural implication

regarding the transport model of V-ATPase. There have been a model that predicts certain conformational changes of a domain in K-ring only when interacting with the stator domain (Fig. 1b). Nevertheless, the results in Fig. 7 clearly exclude the possibility, as the difference spectra are identical between the entire V-ATPase complex and K-ring. It should be noted that the entire V-ATPase complex is intact during the ATR-FTIR measurements, retaining the enzymatic activity (Fig. 6).

While the identical spectra in Fig. 7 provide important structural information related to the transport mechanism, it was entirely unexpected that the ion binding-induced difference spectrum of the K-ring was "too identical" to that of the entire complex (Fig. 7). In the K-ring, one or two subunits are considered to interact with the I subunit for Na^+ or Li^+ ion transport, where R^{573} was proposed to form an ion pair with E^{139} in the K-ring [16, 54]. Therefore, we expected homogeneous structural changes upon ion binding to the K-ring, but the structural changes upon ion binding to the entire V-ATPase complex must be heterogeneous. Although there are spectral deviations between red and blue spectra in Fig. 7, it was concluded that they originate from experimental error such as baseline drift, not the meaningful signals [48]. This implies that protein interaction with the I subunit does not cause large structural changes in the K-ring. This result supports the previously proposed Na^+ transport mechanism by V-ATPase stating that a flip-flop movement of a carboxylate group of E^{139} without large conformational changes in the K-ring accelerates the replacement

of a Na^+ ion in the binding site [17].

5 Mechanistic insights from X-ray structure and vibrational spectroscopy

Murata and his colleagues have previously proposed an ion transport mechanism of V-ATPase based on the crystal structures of ion bound K-ring and the ion binding properties and selectivity of the K-ring [16, 17]. In the model, the clockwise rotation of the K-ring driven by ATP hydrolysis energy in V_1-ATPase, as viewed from the cytoplasm, brings an occupied Na^+-binding site into the K-ring – NtpI interface (Fig. 9a). The proximity of the Na^+ site to the essential R^{573} residue of NtpI produces an electrostatic interaction between R^{573} and E^{139}, disrupting the hydrogen bound network in the Na^+ binding pocket of the K-ring. This results release of the Na^+ ion into the periplasm via a half-channel in NtpI as indicated by the red arrow in Fig. 9b. Further rotation caused by ATP hydrolysis energy in V_1-ATPase (Fig. 9c), which may disrupt the Arg-Glu interaction, results in the binding of a cytoplasmic Na^+ ion as indicated by the blue arrow in Fig. 9d.

While ATR-FTIR study was reported in 2011 [48], the structures of the DCCD-K-ring were determined in the same year [55], which provided further implication about the mechanism. Binding of the DCCD effectively neutralizes the negative charged of the conserved E^{139}, resulting in an ~30 times lower affinity for Na^+ in the binding pocket [55]. The similarity of the Na^+ bound and the Na^+ unbound DCCD-K-ring structures to that of the

wild-type K-ring indicates that there is no global conformational change associated with neutralization of the E^{139} and release of Na^+ from the binding pocket modified with DCCD. The E^{139} neutralized by DCCD is suggested to adopt the same open orientation as it would be through forming an electrostatic interaction with the R^{573} during the ion transport process. Based on these findings, Murata and his colleagues proposed an ion transport mechanism of V-ATPase whereby the ion translocation can be accomplished through changes in the torsion angle of the E^{139} side chain alone, without any other global conformational change at the binding site as shown in Fig. 9 [55].

The ATR-FTIR results are fully consistent with these views based on X-ray crystallography. Identical difference FTIR spectra between the entire complex and K-ring indicate the lack of global conformational change upon association of the K-ring with the stator unit. The identical spectra further suggest that E^{139} does not directly interact with R^{573} in NtpI, where ion-binding site is closed, namely still binding ions, in the resting state of the entire V-ATPase complex. This means the structure in Fig. 9a is the most energetically stable state during the functional cycle of V-ATPase. Further experimental and theoretical efforts will lead to better understanding of the functional cycle of V-ATPase.

6 Conclusion and perspective

Using ion-binding induced difference ATR-FTIR spectroscopy, we showed that sodium

and lithium ion bindings to the K-ring induce deprotonation of E^{139} residue, where structural changes of Y^{68} is also suggested [48]. Transmembrane α-helix conformation is rigid in the presence of sodium and lithium ion, while the release of these ions (= replacement with protons) loosens the α-helical structure. Quantitative analysis suggested that 5–6 peptide backbone groups participate such changes, indicating that the structural alterations are local. Identical difference FTIR spectra upon ion bindings between the entire V-ATPase complex and K-ring indicate that the observed spectral changes monitor local conformational alteration in K-ring. In the entire V-ATPase complex, one or two subunits of the K-ring are considered to interact with the I subunit for Na^+ or Li^+ ion transport, where R^{573} was proposed to form an ion pair with E^{139} in the K-ring. Identical difference FTIR spectra between the entire V-ATPase complex and K-ring strongly suggest that protein interaction with the I subunit does not cause large structural changes in the K-ring. This result supports the previously proposed Na^+ transport mechanism by V-ATPase stating that a flip-flop movement of a carboxylate group of E^{139} without large conformational changes in the K-ring accelerates the replacement of a Na^+ ion in the binding site.

Vibrational spectroscopy cannot determine atomic positions of biomolecules. However, as shown in this review article, it is a powerful method to investigate structural changes of biomolecules in atomic details. In particular, FTIR spectroscopy is a good complimentary technique of X-ray crystallography, which is also presented in this article.

Both X-ray crystallography and ATR-FTIR spectroscopy concluded ion transport mechanism without large conformational changes in the K-ring. Because of recent accelerated structural determination of membrane proteins, ATR-FTIR spectroscopy will be more demanded in future than in the past. Small sample amount needed for ATR-FTIR spectroscopy (~50 μg protein is sufficient for each measurement) is also advantageous for the measurements of the samples, whose preparations are difficult.

Finally recent progresses in ATR-FTIR spectroscopy are noted. Highly accurate detection allows signal acquisition of even a single amino acid. This is also the case for a protein-bound water molecule of cytochrome *c* oxidase [56] and a light-driven chloride pump halorhodopsin [57], where vibrational signal of an internal water molecule was extracted in aqueous solution at ambient temperatures. Measurements of single layered membrane proteins are ideal, whereas normal ATR-FTIR measurements require stacked many layers that accumulate vibrational signals. Surface-enhanced infrared difference absorption spectroscopy (SEIDAS) enables such a single layered measurement [58, 59]. Using this method, structural changes of a membrane photoreceptor were measured under different voltages [60, 61]. Voltage-dependent structural changes have been only reported for photoreceptive proteins, no other general membrane proteins at present, suggesting technical difficulty. Nevertheless, further technical improvement is desired to monitor protein responses of channels, transporters and receptors in the presence of membrane potential.

Many catalytic reactions take place at membrane surface, and membrane extraction of a small G protein by GDP dissociation inhibitor has been recently reported [62]. The same group proposed universal method for protein immobilization on the germanium ATR cell surfaces [63], by which protein structural changes in the protein monolayer upon various stimuli can now be monitored by difference FTIR spectroscopy without metal surface. It should be noted that difference ATR-FTIR spectroscopy is less advantageous to monitor dynamical structural changes upon stimuli, though light stimuli provide good time resolution. However, combination of rapid buffer-exchange system and step-scan time-resolved FTIR spectroscopy allows dynamical protein response upon chloride binding to halorhodopsin [64], which would be a potential method for general membrane proteins. These technical progresses in ATR-FTIR spectroscopy will be used for better understanding of membrane proteins in function.

7 Acknowledgements

This study was partly supported by grants from Japanese Ministry of Education, Culture, Sports, Science, and Technology to H. K. (22247024, 25104009) and Y. F. (22770159, 22018030, 21026016, 21023014) and T. M. (18074003, Targeted Proteins Research Program, and Platform for Drug Discovery, Informatics, and Structural Life Science)

Figure Legends

Fig. 1 Schematic models of ion-transporting mechanism of F-ATPases. The direction of the rotation in these models as shown in black arrows is in the pumping mode but not ATP synthesis mode. Ions, c-ring and a-subunit are shown in blue spheres, grey and green cartoons, respectively. (a) 'two-half-channel' model; side view (b) 'helix swiveling' model; top view from the cytoplasm at the level of the ion-binding sites (c) 'single-channel' model; side view. See text for details.

Fig. 2 Schematic model of *E. hirae* V-ATPase. A side view of the structure model of the V-ATPase complex. ATP hydrolysis induces the rotation of the central stalk with K-ring (indicated with the dotted red line), which causes ion (Na^+ or Li^+) pumping at the interface between the K-ring and NtpI.

Fig. 3 Crystal structures of the K-ring of *E. hirae* V-ATPase. (a) A side view of the K-ring. The red box indicates the location of the ion-binding pocket. (b, c) Close-up views of the ion-binding site of the K-ring (b: Na^+-bound form, c: Li^+-bound form). The Na^+ and Li^+ ions are in light blue and violet, respectively. Dotted lines are Na^+ (or Li^+)-O bounds with distances.

Fig. 4 Experimental setup for stumulus-induced difference ATR-FTIR spectroscopy. (a) Picture of the ATR-FTIR system. (b) The sample compartment. The samples are attached on the ATR cells, which is covered by a glass jacket for maintaining the temperature and introducing buffer solutions to the sample. (c) Buffer exchange system. Exchanging buffer solutions was regulated by a chromatography system with a computer-controlled solenoid valve. Using this system, we are able to obtain the difference FTIR spectra between buffer A and B.

Fig. 5 Ion-binding induced difference infrared spectra of the entire V-ATPase complex. The difference spectra were recorded in the presence and absence of 1 mM NaCl (a: red) or 1mM LiCl (b: blue). (c) The calculated spectra ((a)–(b): green) and the experimentally obtained difference spectrum recorded with 1mM NaCl and LiCl (purple) were compared. (d) Ion binding-induced difference infrared spectra of the entire V-ATPase complex after DCCD treatment (black). The red-colored spectra are reproduced from a. One division of the y-axis corresponds to 0.0015 absorbance unit.

Fig. 6 (a) SDS-PAGE before and after the ATR-FTIR experiment. (b) Na^+-dependent ATPase activity before and after the ATR-FTIR experiment.

Fig. 7 Ion binding-induced difference infrared spectra of the K-ring alone (blue). The red-colored spectra are reproduced from Fig. 5a by changing the amplitude. One division of the y-axis corresponds to 0.0002 absorbance unit.

Fig. 8 (a) Absolute infrared spectrum of the entire complex in the buffer solution (black) and the Na^+ binding induced difference spectrum (red). (b and c) Spectral decomposition of the Na^+ binding spectrum in the amide I region were examined by two methods. The band narrowing of one component and the frequency shifts of two components were assumed in (b) and (c), respectively.

Fig. 9 A model for the ion-transport mechanism of *E.hirae* V-ATPase The model is based on the crystal structures of the K-ring. The views are from the cytoplasm and show the K-ring–NtpI interface at the level of the ion binding sites. Residues involved in ion binding are shown in stick representation. Colors correspond to Fig. 2. NtpI shown in green is in close proximity to the K-ring with the essential R^{573} (blue stick representation), which has two half-channels connecting to the periplasm and cytoplasm, respectively. The ion transport mechanism of V-ATPase is represented by four intermediate states (a-d).

References

[1] J. Chen, Molecular mechanism of the Escherichia coli maltose transporter, Curr. Opin. Struct. Biol., 23 (2013) 492-498.

[2] L. Guan, H.R. Kaback, Lessons from lactose permease, Annu. Rev. Biophys. Biomol. Struct., 35 (2006) 67-91.

[3] V.R.I. Kaila, M.I. Verkhovsky, M. Wikstrom, Proton-Coupled Electron Transfer in Cytochrome Oxidase, Chem Rev, 110 (2010) 7062-7081.

[4] L. Schmitt, R. Tampe, Structure and mechanism of ABC transporters, Curr. Opin. Struct. Biol., 12 (2002) 754-760.

[5] D.L. Stokes, N.M. Green, Structure and function of the calcium pump, Annu. Rev. Biophys. Biomol. Struct., 32 (2003) 445-468.

[6] C. Toyoshima, R. Kanai, F. Cornelius, First crystal structures of Na+,K+-ATPase: new light on the oldest ion pump, Structure, 19 (2011) 1732-1738.

[7] M. Forgac, Vacuolar ATPases: rotary proton pumps in physiology and pathophysiology, Nat. Rev. Mol. Cell Biol., 8 (2007) 917-929.

[8] W. Junge, H. Lill, S. Engelbrecht, ATP synthase: an electrochemical transducer with rotatory mechanics, Trends Biochem. Sci., 22 (1997) 420-423.

[9] V.K. Rastogi, M.E. Girvin, Structural changes linked to proton translocation by subunit c of the ATP synthase, Nature, 402 (1999) 263-268.

[10] G. Kaim, U. Matthey, P. Dimroth, Mode of interaction of the single a subunit with the multimeric c subunits during the translocation of the coupling ions by F1F0 ATPases, EMBO J., 17 (1998) 688-695.

[11] P. Dimroth, C. von Ballmoos, T. Meier, Catalytic and mechanical cycles in F-ATP synthases. Fourth in the Cycles Review Series, EMBO Rep., 7 (2006) 276-282.

[12] O.D. Vincent, B.E. Schwem, P.R. Steed, W. Jiang, R.H. Fillingame, Fluidity of structure

and swiveling of helices in the subunit c ring of *Escherichia coli* ATP synthase as revealed by cysteine-cysteine cross-linking, J. Biol. Chem., 282 (2007) 33788-33794.

[13] T. Murata, M. Kawano, K. Igarashi, I. Yamato, Y. Kakinuma, Catalytic properties of Na(+)-translocating V-ATPase in *Enterococcus hirae*, Biochim Biophys Acta, 1505 (2001) 75-81.

[14] T. Murata, I. Yamato, K. Igarashi, Y. Kakinuma, Intracellular Na+ regulates transcription of the ntp operon encoding a vacuolar-type Na+-translocating ATPase in *Enterococcus hirae*, J. Biol. Chem., 271 (1996) 23661-23666.

[15] Y. Kakinuma, I. Yamato, T. Murata, Structure and function of vacuolar Na+-translocating ATPase in *Enterococcus hirae*, J. Bioenerg. Biomembr., 31 (1999) 7-14.

[16] T. Murata, I. Yamato, Y. Kakinuma, A.G. Leslie, J.E. Walker, Structure of the rotor of the V-Type Na+-ATPase from *Enterococcus hirae*, Science, 308 (2005) 654-659.

[17] T. Murata, I. Yamato, Y. Kakinuma, M. Shirouzu, J.E. Walker, S. Yokoyama, S. Iwata, Ion binding and selectivity of the rotor ring of the Na+-transporting V-ATPase, Proc. Natl. Acad. Sci. USA, 105 (2008) 8607-8612.

[18] J. Breton, Fourier transform infrared spectroscopy of primary electron donors in type I photosynthetic reaction centers, Biochim Biophys Acta, 1507 (2001) 180-193.

[19] Y. Furutani, H. Kandori, Hydrogen-bonding changes of internal water molecules upon the actions of microbial rhodopsins studied by FTIR spectroscopy, Biochim Biophys Acta, 1837 (2014) 598-605.

[20] K. Gerwert, Molecular reaction mechanisms of proteins monitored by time-resolved FTIR-spectroscopy, Biol. Chem., 380 (1999) 931-935.

[21] F. Siebert, Infrared-Spectroscopy Applied to Biochemical and Biological Problems, Method Enzymol, 246 (1995) 501-526.

[22] Y. Furutani, M. Shibata, H. Kandori, Strongly hydrogen-bonded water molecules in the

Schiff base region of rhodopsins, Photochem. Photobiol. Sci., 4 (2005) 661-666.

[23] H. Kandori, Role of internal water molecules in bacteriorhodopsin, Biochim Biophys Acta, 1460 (2000) 177-191.

[24] T. Noguchi, FTIR detection of water reactions in the oxygen-evolving centre of photosystem II, Philos. Trans. R Soc. Lond. B Biol. Sci., 363 (2008) 1189-1194; discussion 1194-1185.

[25] W. Mantele, Reaction-induced infrared difference spectroscopy for the study of protein function and reaction mechanisms, Trends. Biochem. Sci., 18 (1993) 197-202.

[26] R.M. Nyquist, K. Ataka, J. Heberle, The molecular mechanism of membrane proteins probed by evanescent infrared waves, Chembiochem, 5 (2004) 431-436.

[27] P.R. Rich, M. Iwaki, Methods to probe protein transitions with ATR infrared spectroscopy, Mol. Biosyst., 3 (2007) 398-407.

[28] M. Iwaki, L. Giotta, A.O. Akinsiku, H. Schagger, N. Fisher, J. Breton, P.R. Rich, Redox-induced transitions in bovine cytochrome bc_1 complex studied by perfusion-induced ATR-FTIR spectroscopy, Biochemistry, 42 (2003) 11109-11119.

[29] M. Iwaki, A. Puustinen, M. Wikstrom, P.R. Rich, ATR-FTIR spectroscopy and isotope labeling of the PM intermediate of *Paracoccus denitrificans* cytochrome *c* oxidase, Biochemistry, 43 (2004) 14370-14378.

[30] A. Marechal, M. Iwaki, P.R. Rich, Structural changes in cytochrome c oxidase induced by binding of sodium and calcium ions: an ATR-FTIR study, J. Am. Chem. Soc., 135 (2013) 5802-5807.

[31] R.M. Nyquist, D. Heitbrink, C. Bolwien, R.B. Gennis, J. Heberle, Direct observation of protonation reactions during the catalytic cycle of cytochrome *c* oxidase, Proc. Natl. Acad. Sci. USA, 100 (2003) 8715-8720.

[32] F. Scheirlinckx, V. Raussens, J.M. Ruysschaert, E. Goormaghtigh, Conformational

changes in gastric H+/K+-ATPase monitored by difference Fourier-transform infrared spectroscopy and hydrogen/deuterium exchange, Biochem. J., 382 (2004) 121-129.

[33] J.E. Baenziger, K.W. Miller, K.J. Rothschild, Fourier transform infrared difference spectroscopy of the nicotinic acetylcholine receptor: evidence for specific protein structural changes upon desensitization, Biochemistry, 32 (1993) 5448-5454..

[34] J.E. Baenziger, J.P. Chew, Desensitization of the nicotinic acetylcholine receptor mainly involves a structural change in solvent-accessible regions of the polypeptide backbone, Biochemistry, 36 (1997) 3617-3624.

[35] S.E. Ryan, C.N. Demers, J.P. Chew, J.E. Baenziger, Structural effects of neutral and anionic lipids on the nicotinic acetylcholine receptor. An infrared difference spectroscopy study., J. Biol. Chem., 271 (1996) 24590-24597.

[36] J. le Coutre, E. Turk, H.R. Kaback, E.M. Wright, Ligand-induced differences in secondary structure of the *Vibrio parahaemolyticus* Na+/galactose cotransporter, Biochemistry, 41 (2002) 8082-8086.

[37] S. Doki, H.E. Kato, N. Solcan, M. Iwaki, M. Koyama, M. Hattori, N. Iwase, T. Tsukazaki, Y. Sugita, H. Kandori, S. Newstead, R. Ishitani, O. Nureki, Structural basis for dynamic mechanism of proton-coupled symport by the peptide transporter POT, Proc. Natl. Acad. Sci. USA, 110 (2013) 11343-11348.

[38] M. Iwaki, N.P. Cotton, P.G. Quirk, P.R. Rich, J.B. Jackson, Molecular recognition between protein and nicotinamide dinucleotide in intact, proton-translocating transhydrogenase studied by ATR-FTIR Spectroscopy, J. Am. Chem. Soc., 128 (2006) 2621-2629.

[39] S.J. Whitehead, M. Iwaki, N.P. Cotton, P.R. Rich, J.B. Jackson, Inhibition of proton-transfer steps in transhydrogenase by transition metal ions, Biochim Biophys Acta, 1787 (2009) 1276-1288.

[40] M. Granell, X. Leon, G. Leblanc, E. Padros, V.A. Lorenz-Fonfria, Structural insights into the activation mechanism of melibiose permease by sodium binding, Proc. Natl. Acad. Sci. USA, 107 (2010) 22078-22083.

[41] Y. Lin, O. Fuerst, M. Granell, G. Leblanc, V. Lorenz-Fonfria, E. Padros, The substitution of Arg149 with Cys fixes the melibiose transporter in an inward-open conformation, Biochim Biophys Acta, 1828 (2013) 1690-1699.

[42] V.A. Lorenz-Fonfria, M. Granell, X. Leon, G. Leblanc, E. Padros, In-plane and out-of-plane infrared difference spectroscopy unravels tilting of helices and structural changes in a membrane protein upon substrate binding, J. Am. Chem. Soc., 131 (2009) 15094-15095.

[43] J. Guijarro, M. Engelhard, F. Siebert, Anion uptake in halorhodopsin from *Natromonas pharaonis* studied by FTIR spectroscopy: consequences for the anion transport mechanism, Biochemistry, 45 (2006) 11578-11588.

[44] K. Inoue, H. Ono, R. Abe-Yoshizumi, S. Yoshizawa, H. Ito, K. Kogure, H. Kandori, A light-driven sodium ion pump in marine bacteria, Nat. Commun., 4 (2013) 1678.

[45] Y. Kitade, Y. Furutani, N. Kamo, H. Kandori, Proton release group of *pharaonis* phoborhodopsin revealed by ATR-FTIR spectroscopy, Biochemistry, 48 (2009) 1595-1603.

[46] Y. Sudo, Y. Kitade, Y. Furutani, M. Kojima, S. Kojima, M. Homma, H. Kandori, Interaction between Na(+) ion and carboxylates of the PomA-PomB stator unit studied by ATR-FTIR spectroscopy, Biochemistry, 48 (2009) 11699-11705.

[47] Y. Furutani, H. Shimizu, Y. Asai, T. Fukuda, S. Oiki, H. Kandori, ATR-FTIR Spectroscopy Revealing the Different Vibrational Modes of the Selectivity Filter Interacting with K+ and Na+ in the Open and Collapsed Conformations of the KcsA Potassium Channel, J. Phys. Chem. Lett., 3 (2012) 3806-3810.

[48] Y. Furutani, T. Murata, H. Kandori, Sodium or Lithium Ion-Binding-Induced Structural Changes in the K-Ring of V-ATPase from Enterococcus hirae Revealed by ATR-FTIR

Spectroscopy, J. Am. Chem. Soc., 133 (2011) 2860-2863.

[49] T. Murata, K. Igarashi, Y. Kakinuma, I. Yamato, Na+ binding of V-type Na+-ATPase in *Enterococcus hirae*, J. Biol. Chem., 275 (2000) 13415-13419.

[50] G.B. Deacon, R.J. Phillips, Relationships between the carbon-oxygen stretching frequencies of carboxylato complexes and the type of carboxylate coordination., Coord. Chem. Rev., 33 (1980) 227-250.

[51] M. Nara, H. Torii, M. Tasumi, Correlation between the vibrational frequencies of the carboxylate group and the types of its coordination to a metal ion: An ab Initio molecular orbital study, J. Phys. Chem., 100 (1996) 19812-19817.

[52] A. Barth, The infrared absorption of amino acid side chains, Prog. Biophys. Mol. Biol., 74 (2000) 141-173.

[53] B. Nie, J. Stutzman, A. Xie, A vibrational spectral maker for probing the hydrogen-bonding status of protonated Asp and Glu residues, Biophys. J., 88 (2005) 2833-2847.

[54] T. Murata, I. Yamato, Y. Kakinuma, Structure and mechanism of vacuolar Na+-translocating ATPase from *Enterococcus hirae*, J. Bioenerg. Biomembr., 37 (2005) 411-413.

[55] K. Mizutani, M. Yamamoto, K. Suzuki, I. Yamato, Y. Kakinuma, M. Shirouzu, J.E. Walker, S. Yokoyama, S. Iwata, T. Murata, Structure of the rotor ring modified with N,N'-dicyclohexylcarbodiimide of the Na+-transporting vacuolar ATPase, Proc. Natl. Acad. Sci. USA, 108 (2011) 13474-13479.

[56] A. Marechal, P.R. Rich, Water molecule reorganization in cytochrome *c* oxidase revealed by FTIR spectroscopy, Proc. Natl. Acad. Sci. USA, 108 (2011) 8634-8638.

[57] T. Fukuda, K. Muroda, H. Kandori, Detection of a protein-bound water vibration of halorhodopsin in aqueous solution, BIOPHYSICS, 9 (2013) 167-172.

[58] K. Ataka, F. Giess, W. Knoll, R. Naumann, S. Haber-Pohlmeier, B. Richter, J. Heberle, Oriented attachment and membrane reconstitution of His-tagged cytochrome c oxidase to a gold electrode: in situ monitoring by surface-enhanced infrared absorption spectroscopy, J. Am. Chem. Soc., 126 (2004) 16199-16206.

[59] K. Ataka, J. Heberle, Electrochemically induced surface-enhanced infrared difference absorption (SEIDA) spectroscopy of a protein monolayer, J. Am. Chem. Soc., 125 (2003) 4986-4987.

[60] X. Jiang, M. Engelhard, K. Ataka, J. Heberle, Molecular impact of the membrane potential on the regulatory mechanism of proton transfer in sensory rhodopsin II, J. Am. Chem. Soc., 132 (2010) 10808-10815.

[61] X. Jiang, E. Zaitseva, M. Schmidt, F. Siebert, M. Engelhard, R. Schlesinger, K. Ataka, R. Vogel, J. Heberle, Resolving voltage-dependent structural changes of a membrane photoreceptor by surface-enhanced IR difference spectroscopy, Proc. Natl. Acad. Sci. USA, 105 (2008) 12113-12117.

[62] K. Gavriljuk, A. Itzen, R.S. Goody, K. Gerwert, C. Kotting, Membrane extraction of Rab proteins by GDP dissociation inhibitor characterized using attenuated total reflection infrared spectroscopy, Proc. Natl. Acad. Sci. USA, 110 (2013) 13380-13385.

[63] J. Schartner, J. Guldenhaupt, B. Mei, M. Rogner, M. Muhler, K. Gerwert, C. Kotting, Universal method for protein immobilization on chemically functionalized germanium investigated by ATR-FTIR difference spectroscopy, J. Am. Chem. Soc., 135 (2013) 4079-4087.

[64] Y. Furutani, T. Kimura, K. Okamoto, Development of a rapid Buffer-exchange system for time-resolved ATR-FTIR spectroscopy with the step-scan mode, BIOPHYSICS, 9 (2013) 123-129.

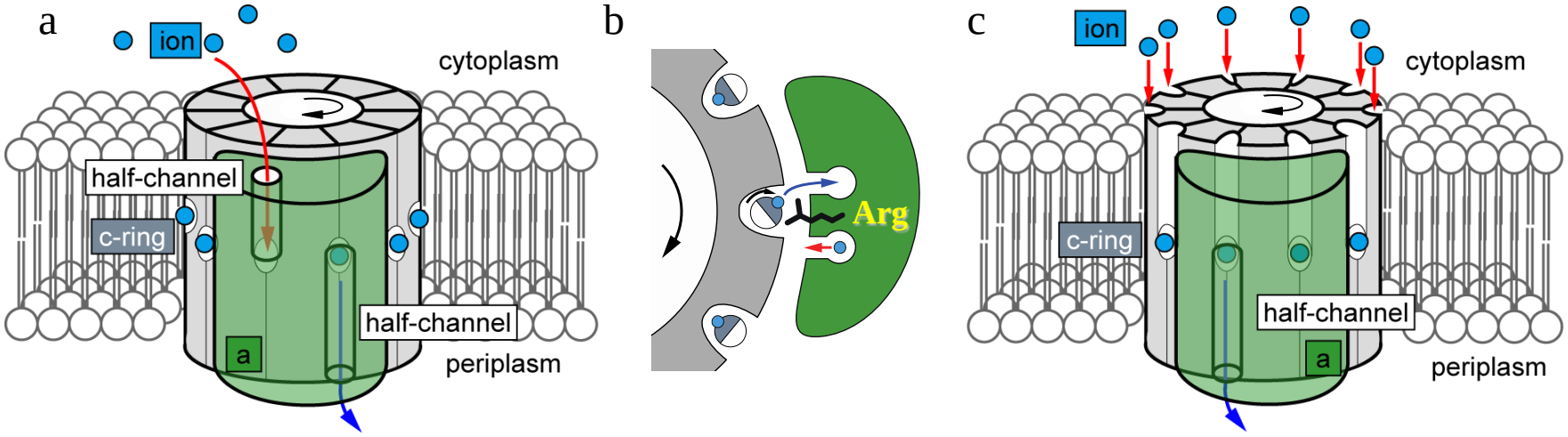
a
ion
cytoplasm
half-channel
c-ring
half-channel
a
periplasm
b
Arg
c
ion
cytoplasm
c-ring
half-channel
a
periplasm

Fig. 1

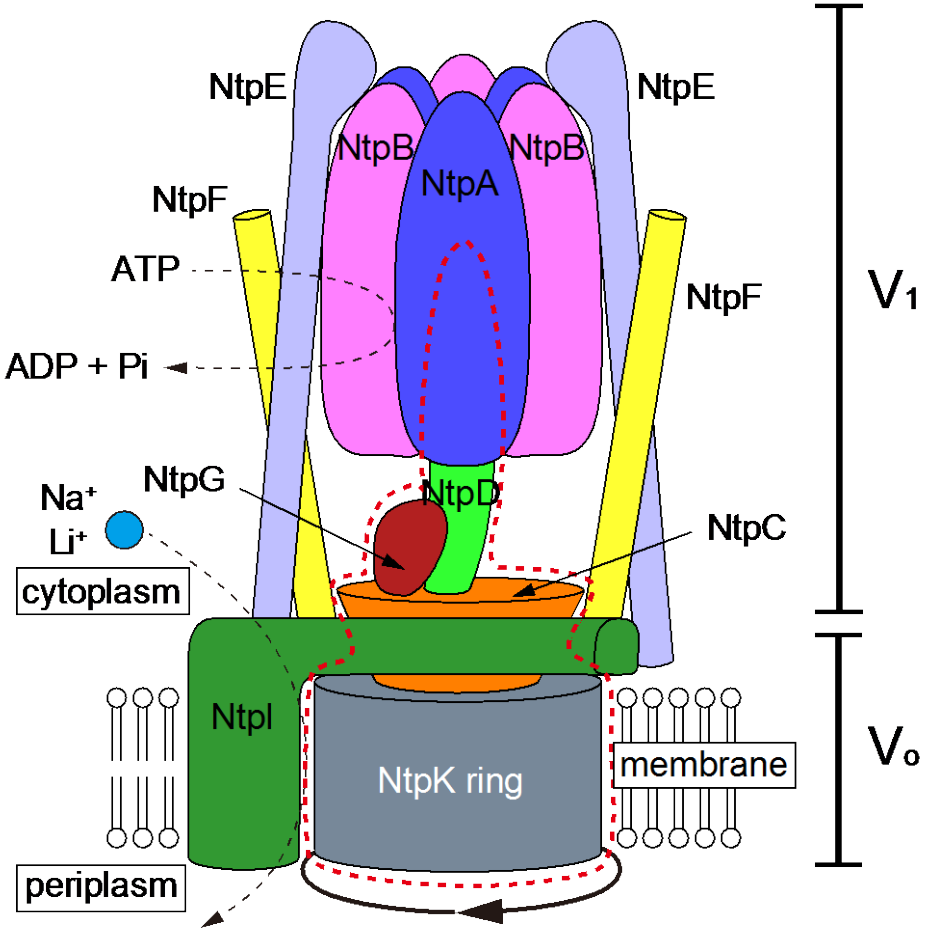
NtpE
NtpE
NtpB
NtpB
NtpA
NtpF
ATP
NtpF
ADP + Pi
V1
NtpG
Na+
Li+
NtpD
NtpC
cytoplasm
NtpI
NtpK ring
membrane
Vo
periplasm

Fig. 2

a

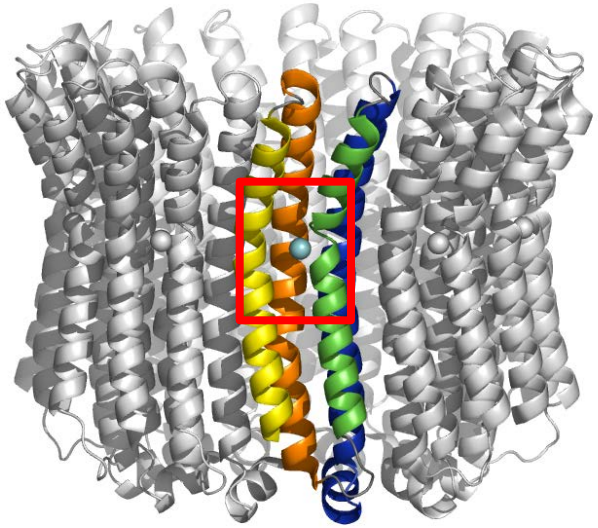

b

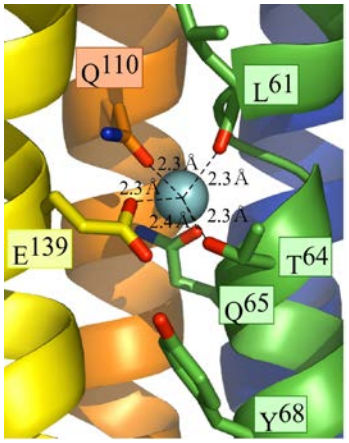
Q110
L61
2.3 Å
2.3 Å
2.3 Å
2.4 Å
2.3 Å
E139
T64
Q65
Y68

c

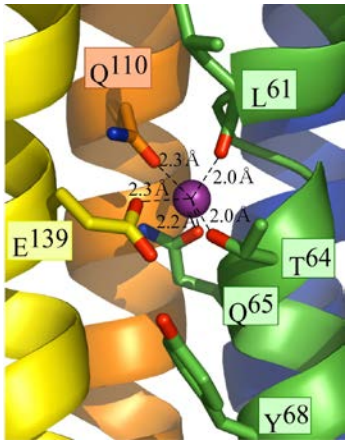
Q110
L61
2.3 Å
2.0 Å
2.3 Å
2.2 Å
2.0 Å
E139
T64
Q65
Y68

Fig. 3

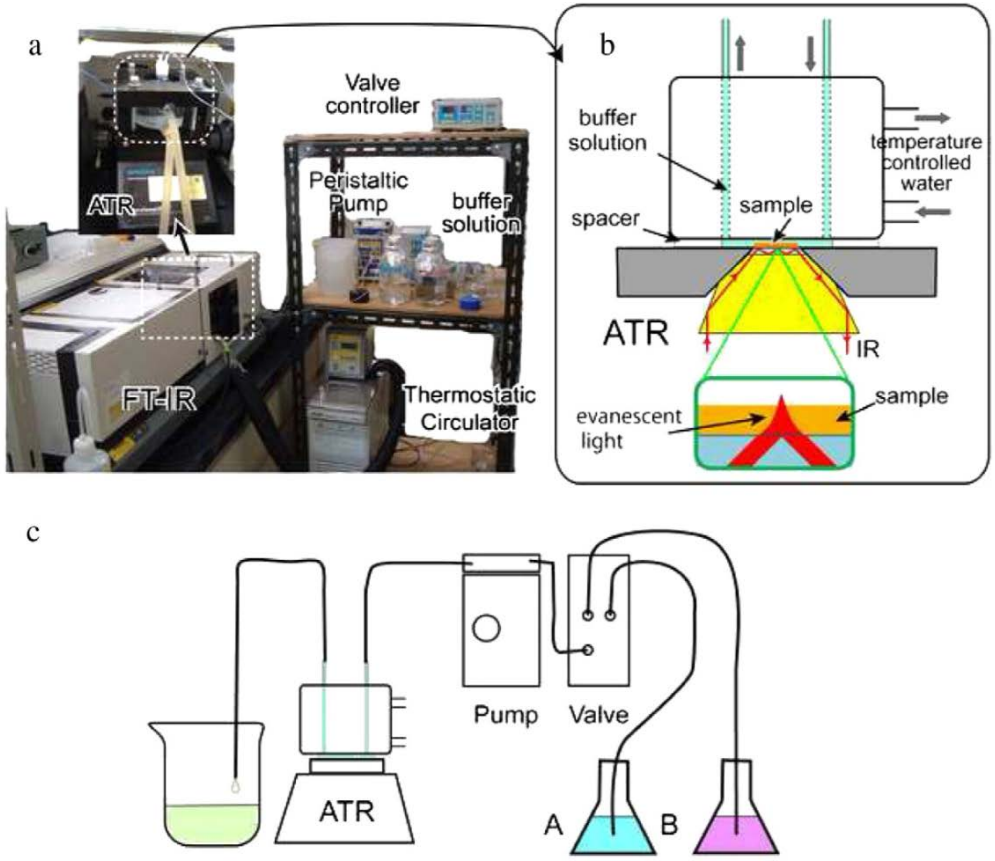
a
ATR
Valve
controller
Peristaltic
Pump
buffer
solution
FT-IR
Thermostatic
Circulator
b
buffer
solution
temperature
controlled
water
spacer
sample
ATR
IR
sample
evanescent
light
c
Pump
Valve
ATR
A
B

Fig. 4

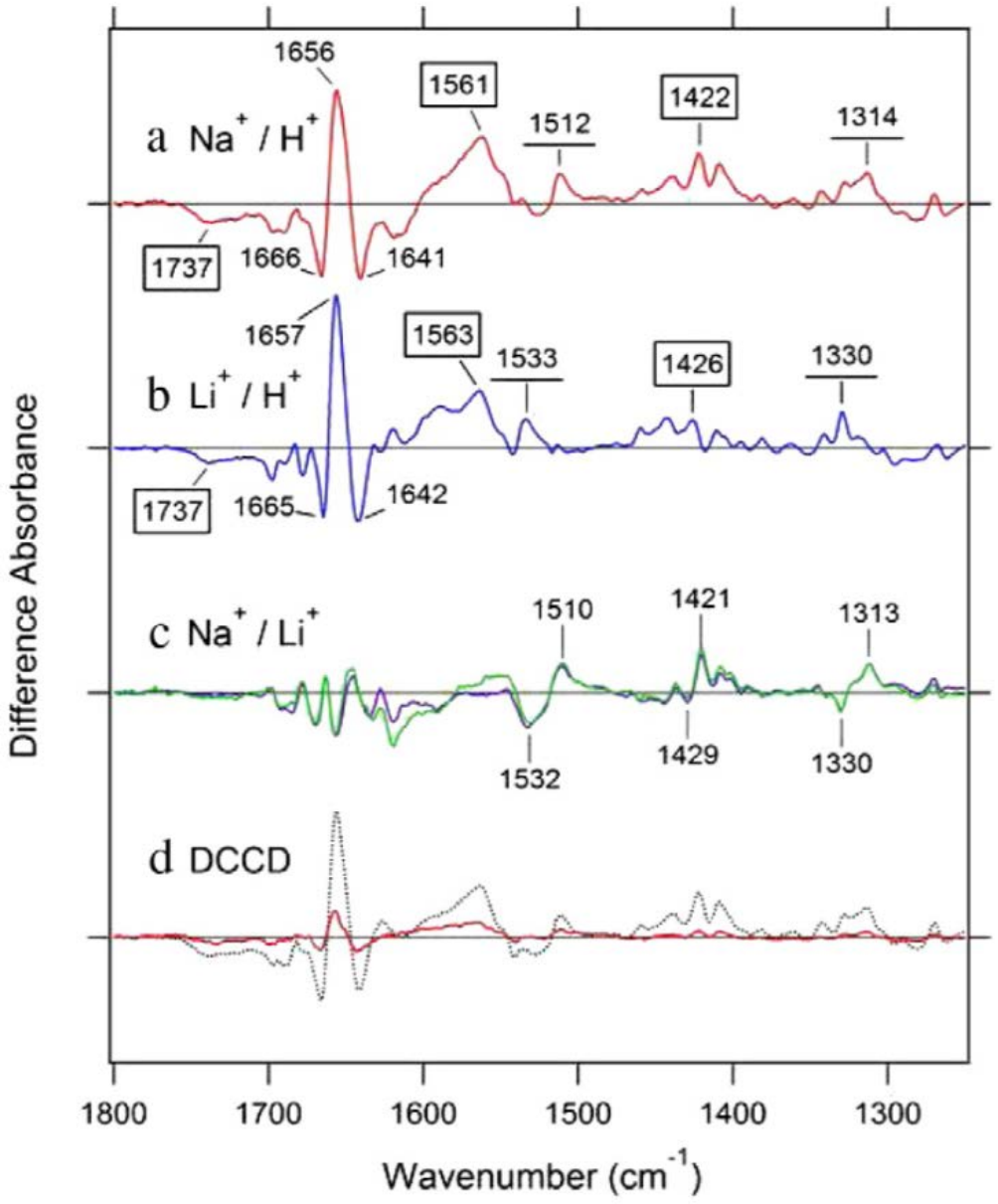
a Na+ / H+
1656
1561
1512
1422
1314
1737
1666
1641
b Li+ / H+
1657
1563
1533
1426
1330
1737
1665
1642
c Na+ / Li+
1510
1421
1313
1532
1429
1330
d DCCD
Difference Absorbance
1800
1700
1600
1500
1400
1300
Wavenumber (cm-1)

Fig. 5

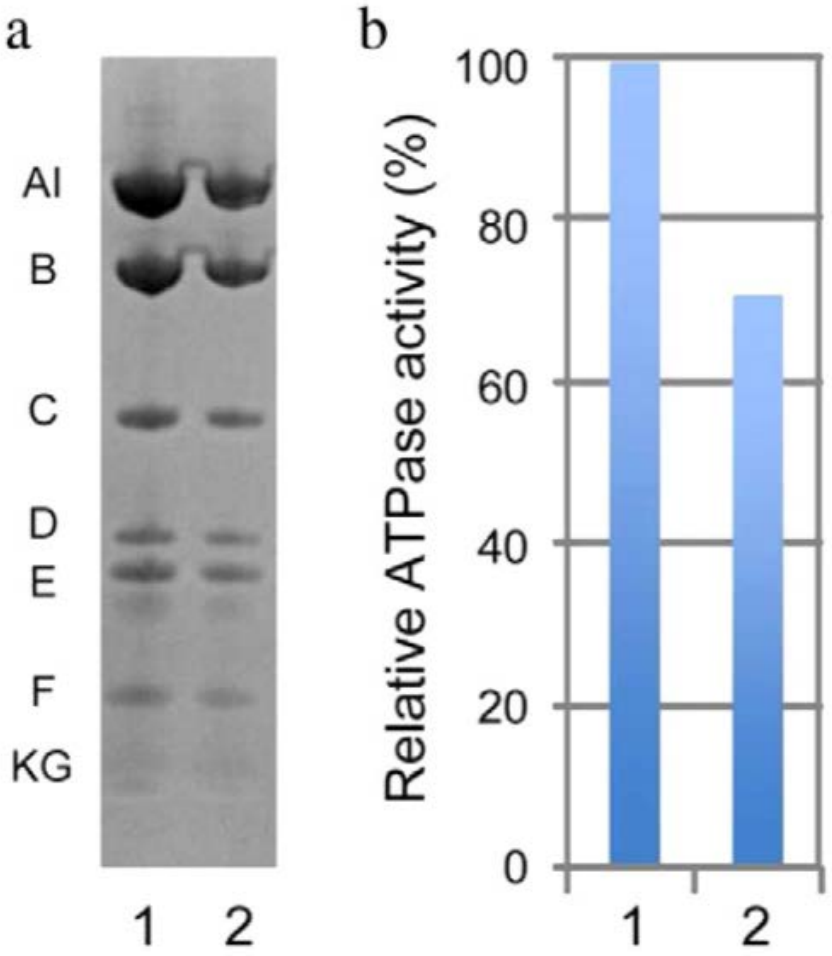

Fig. 6

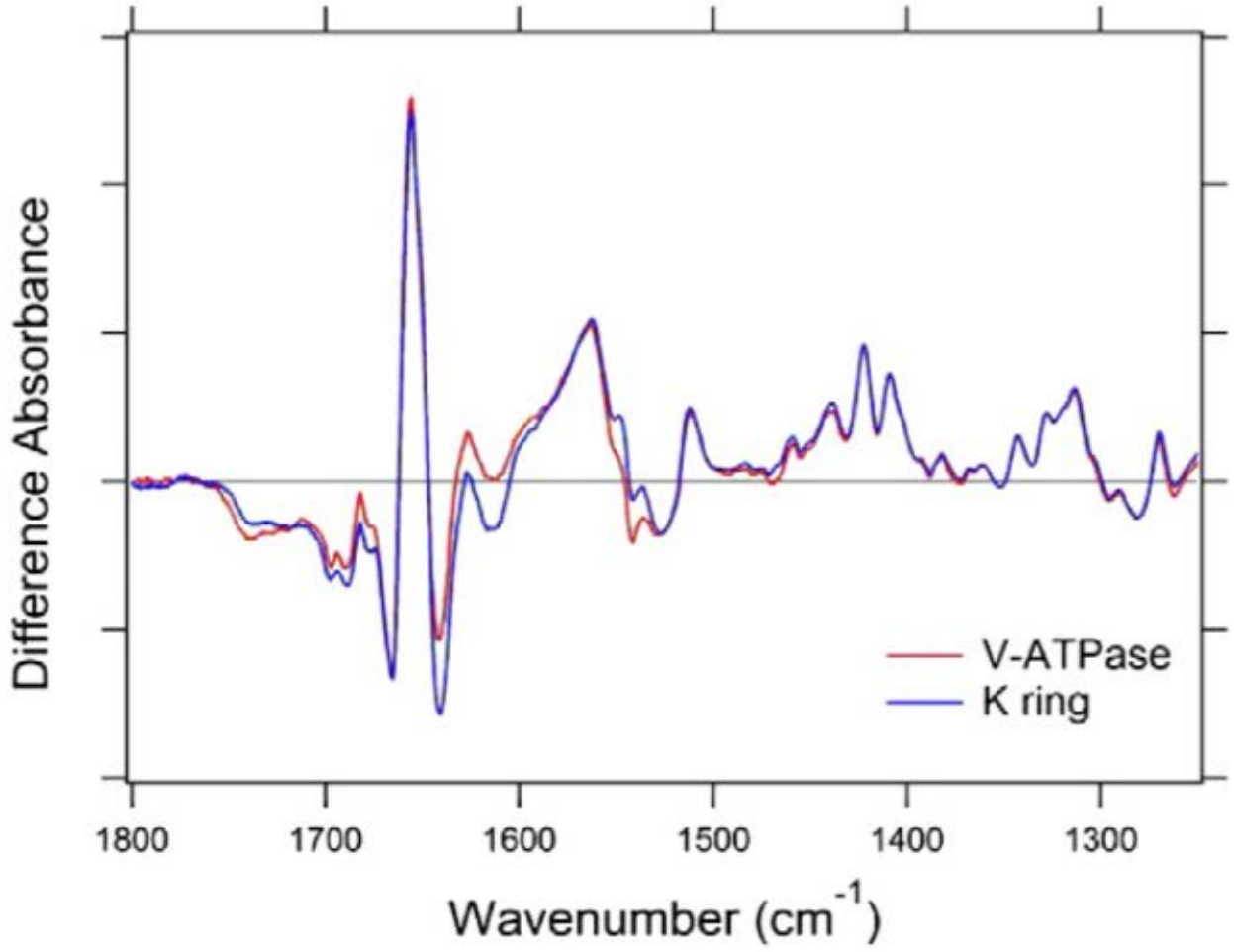
Difference Absorbance
V-ATPase
K ring
1800
1700
1600
1500
1400
1300
Wavenumber (cm-1)

Fig. 7

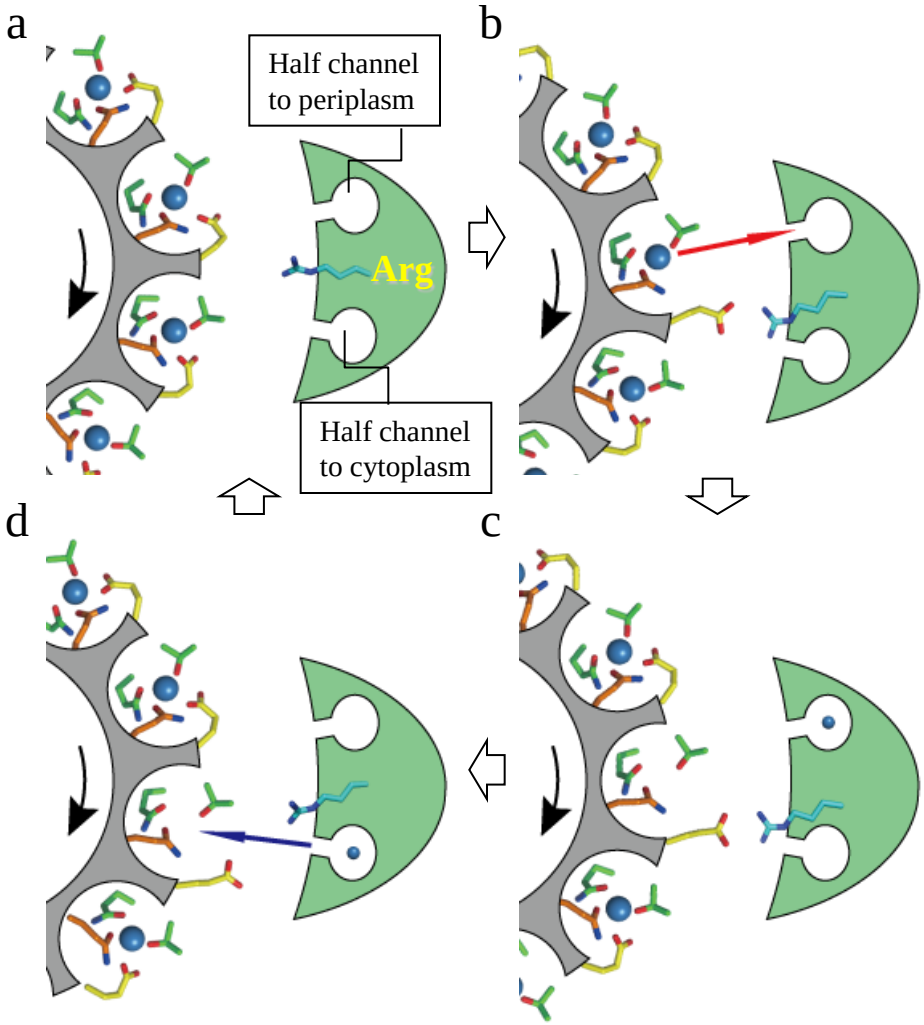
a
b
c
d
Half channel
to periplasm
Arg
Half channel
to cytoplasm

Fig. 8